

# Calculating the $Q\bar{Q}$ potential in (2+1)-dimensional light-front QCD

M. Burkardt and B. Klindworth

*Department of Physics, New Mexico State University, Las Cruces, New Mexico 88003-0001*

(Received 10 January 1996; revised manuscript received 20 August 1996)

Pure glue QCD is formulated on a (2+1)-dimensional transverse lattice, using discrete light-front quantization. The transverse component of the gauge fields is taken to be compact, but in a linearized approximation with an effective potential. The (rest-frame)  $Q\bar{Q}$  potential is evaluated numerically using Lanczos matrix diagonalization. We first discuss the strong coupling limit analytically and then present numerical results beyond the strong coupling limit. The physical origin of confinement on a transverse lattice depends on the orientation of the external charges: For longitudinally separated charges, confinement arises from the instantaneous Coulomb interaction and for transversely separated quarks a string of link-fields forms. In the general case one obtains a superposition of both effects. Despite the asymmetry in the microscopic mechanism, already a very simple ansatz for the effective link-field potential provides an almost rotationally invariant  $Q\bar{Q}$  potential. The momentum carried by the glue depends strongly on the orientation of the external charges, which might have observable consequences. [S0556-2821(97)00602-4]

PACS number(s): 12.38.Gc

## I. INTRODUCTION

Light-cone coordinates [1] are the natural coordinates for describing high-energy scattering [2–5]. The immense wealth of data on nucleon and nucleus structure functions thus strongly motivates one to understand QCD on the light cone. The transverse lattice formulation of QCD [6–9] is a particularly promising approach towards this goal. Among the most appealing features of this approach to light-front QCD is that confinement emerges naturally in the limit of large lattice spacing [6,10].

In the transverse lattice formulation, the transverse space directions are discretized, while the longitudinal [i.e., the  $x^\pm \equiv (x^0 \pm x^3)/\sqrt{2}$ ] directions are kept continuous (Fig. 1). While this seems to be a natural procedure when quantizing on the light front, the procedure is obviously not manifestly rotationally invariant and one might ask oneself whether rotational invariance is recovered in the continuum limit [11]. This issue becomes even more relevant, when one considers “practical” calculations (in contrast to the infinitely complicated continuum limit), i.e., calculations where the lattice spacing is not necessarily infinitesimally small because of numerical limitations or where one makes approximations on top of the discretization.

In this paper, we will consider one specific observable, namely the rest-frame potential energy of an (infinitely heavy)  $Q\bar{Q}$  pair coupled to the gluon system. As has been shown in Ref. [13], this observable can be extracted from a light-front Hamiltonian by considering a  $Q\bar{Q}$  pair which moves with uniform velocity and where the separation between the quark and the antiquark is kept fixed (the corresponding formalism is briefly summarized in Appendix A).

After setting the general formalism, we will proceed to calculate the  $Q\bar{Q}$  potential away from the strong coupling limit. The main issues there are to find out whether linear confinement persists and whether rotational invariance for the potential is being restored.

## II. THE HAMILTONIAN

The light-front Hamiltonian for compact QCD on a transverse lattice has been introduced in Ref. [6]. For pure glue QCD in 2+1 dimensions one finds

$$P^- = c_g \sum_n \int dx^- \int dy^- : \text{tr} [J_n(x^-) |x^- - y^-| J_n(y^-)] : + V_{\text{eff}}(U), \tag{2.1}$$

where

$$J_n = U_n^\dagger \vec{\partial} U_n - U_{n+1}^\dagger \vec{\partial} U_{n+1} \tag{2.2}$$

and  $U_n$  are the link fields, which are quantized matrix fields and satisfy the usual commutation relations. Ideally, one would like to work with  $U_n \in \text{SU}(N)$ , but in practice this is very complicated [9] so in practice one may prefer to work with an unconstrained complex matrix field and instead add an effective constraint term  $V_{\text{eff}}(U)$  to the light-front (LF) Hamiltonian. In the case of  $N \rightarrow \infty$ , in the classical limit,  $V_{\text{eff}}(U)$  can be taken of the form

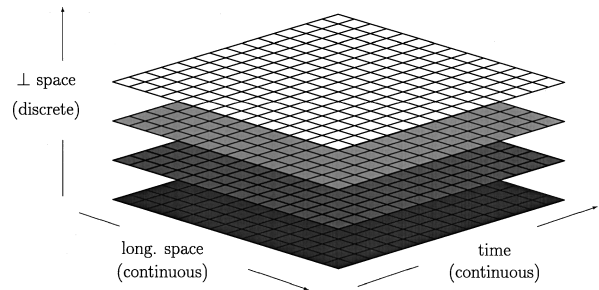


FIG. 1. Space-time view of a transverse lattice.

$$V_{\text{eff}}^{\text{cl}}(U) = c_2 \sum_n \text{tr}: [U_n^\dagger U_n]: + c_4 \sum_n \text{tr}: [U_n^\dagger U_n U_n^\dagger U_n]:, \quad (2.3)$$

where  $c_2 = -2c_4$  and  $c_4 \rightarrow \infty$ , which provides an effective potential that is minimized for  $U_n \in U(N)$ . In the  $N \rightarrow \infty$  limit, the difference between  $U(N)$  and  $SU(N)$  is irrelevant and Eq. (2.3) is thus suitable for enforcing the  $SU(N)$  constraint in the classical limit. One might be tempted to try a similar ansatz for the LF quantized case. There are several reasons why a different form for the effective potential is more useful. First, if one still attempts to work with an effective potential of the above form then physical states would necessarily look extremely complicated, which has to do with the fact that the above ansatz for the effective potential corresponds to working close to the continuum limit. Thus even if the ansatz in Eq. (2.3) would work in principle, it would most likely not be very practical.

However, since a ‘‘Mexican hat’’ potential corresponds to a situation where one is working with the false vacuum, it is questionable whether a physical situation where a particle runs at the bottom of a Mexican hat can be described at all by a LF Hamiltonian, using degrees of freedom expanded around the origin.

For these two reasons, it makes more sense not to consider  $U_n$  as the *bare* link field, but instead think of it as some kind of *blocked* or *smeared* variable. The blocking has several consequences. First, the  $SU(N)$  constraint gets relaxed which reflects itself in the fact that the effective potential is no longer just a narrow valley [12]. Second, using smeared variables, it might be easier to cover large physical distances with only few degrees of freedom. The price one has to pay for these advantages is that the effective potential gets more complex and in general more terms are necessary than shown in Eq. (2.3). In Ref. [24] an attempt has been made to fit the effective potential to the glueball spectrum by making an ansatz which includes all operators up to dimension four. Since this work is a first study of the rest-frame  $Q\bar{Q}$  potential and, as we will discuss below, the  $Q\bar{Q}$  potential turns out to be rather insensitive to terms of dimension greater than two in  $V_{\text{eff}}(U)$ , we will instead only consider a much simpler ansatz in the following and keep only the quadratic term

$$V_{\text{eff}}(U) \approx c_2 \text{tr}(U^\dagger U). \quad (2.4)$$

### III. NUMERICAL PROCEDURE AND RESULTS

Once one has made an ansatz for the Hamiltonian, one needs to find approximate solutions. In this work, we will employ discrete light-cone quantization (DLCQ) [14] for this purpose, i.e., on each link the gauge field  $U_n$  will be expanded in a plane wave basis of complex matrix fields. For simplicity, zero-mode degrees of freedom will be omitted in this procedure, but we impose a color singlet constraint at each site:

$$Q_n |\text{phys}\rangle \equiv \int dx^- J_n(x^-) |\text{phys}\rangle = 0, \quad (3.1)$$

which is known to result after eliminating zero-mode degrees of freedom in the limit of a large longitudinal interval [15].<sup>1</sup> In the large  $N$  limit, the color singlet constraint is easily satisfied by using a basis of states that can be written as traces over color indices. This has been shown in Ref. [6] and will be used in this paper.

To some extent, one can justify the omission of zero modes in the sense of Refs. [16–21] by formulating the theory in terms of an effective light-front Hamiltonian, where high-energy degrees of freedom have been integrated out. While this procedure certainly takes care of some of the zero-mode dynamics, it is not clear whether this allows one to completely omit zero modes as dynamical degrees of freedom. Therefore, one should regard the omission of zero modes (as dynamical degrees of freedom) in this paper as an *ad hoc* approximation which is applied to make the problem simpler. Including dynamical zero modes is one of the many possible improvements that one could consider as an extension of this work [22].

In principle, there can be an arbitrary number of gluon quanta on each of the links of the transverse lattice. The only constraint is the above-mentioned color singlet requirement on each site. In order to simplify the numerical calculation, we will first calculate the  $Q\bar{Q}$  potential under the (*ad hoc*) approximation that each link contains at most one gluon quantum. In combination with the color singlet requirement this implies that a  $Q\bar{Q}$  pair separated by  $N$  transverse links will be connected by exactly  $N$  gluons—one on each link in between.<sup>2</sup> The reason for doing this approximation is that it allows one to illustrate the confinement mechanism on the LF more clearly. Further below we will show results that do not make use of this approximation.

The physical meaning of the *one gluon per link* approximation is as follows: In the limit of large gluon masses (=large lattice spacings) a  $Q\bar{Q}$  pair is connected by a static (no fluctuations) chain of gluons. As the gluon mass gets smaller, the string starts fluctuating. Fluctuations where the string moves longitudinally with respect to the straight line connecting the  $Q\bar{Q}$  pair correspond to excitations which do not change the number of link fields. Those are included in the above approximation. Fluctuations which are excluded in the above approximation are the ones where the string gets deformed transversely so strongly that it winds forth and back in the transverse direction. If one wants an exact solution to QCD, all fluctuations must be included. However, as a first step beyond the (static) heavy gluon limit, it makes sense to include only the ‘‘motion’’ of the gluons first but not creation and annihilation of additional gluons. Note that if one were to work close to the continuum limit then such an approximation would not make sense. However, since we consider the  $U$ ’s as blocked variables, which correspond to

<sup>1</sup>Note that even though this has been shown only for  $(1+1)$ -dimensional gauge theories in Ref. [15], the result can be used here since QCD on a transverse lattice is formally equivalent to a large number of coupled  $(1+1)$ -dimensional field theories.

<sup>2</sup>Without this approximation, this would be the minimal configuration, i.e., any physical state subject to the color singlet constraint at each site will have at least this number of gluons.

rather rigid degrees of freedom, it is not completely unreasonable to assume that pair creation is suppressed in ground state configurations.

The general formalism for calculating the (rest-frame)  $Q\bar{Q}$  potential within the light-front framework has been discussed in detail in Ref. [13] and the reader is strongly encouraged to consult these works for details. In the following we will only present the explicit integral equations that one obtains for the coupled  $Q\bar{Q}$ -glue system. If the quark and the anti-quark are on the same site, with longitudinal separation  $x^-$ , the calculation is trivial since the ‘‘integral equation’’ collapses into one single equation:

$$P^- = G^2 \frac{\pi}{2} |x^-|, \quad (3.2)$$

where  $G^2 = g^2 N / 2\pi$ .  $g$  carries dimensions of mass. The factor  $N$  arises from traces over matrices. The naive continuum limit is related to the coupling constant  $g_0$  in the Lagrangian of (2+1)-dimensional QCD (QCD<sub>2+1</sub>) via  $g^2 \propto g_0^2 / a$ , where  $a$  is the transverse lattice spacing, which is why the coupling has this unusual dimension. As has been shown in Ref. [13],  $x^-$  is related to the longitudinal separation of the  $Q\bar{Q}$  pair in its rest frame  $x_L$  via

$$x_L = x^- v^+, \quad (3.3)$$

where  $v^\mu$  is the velocity vector of the  $Q\bar{Q}$  pair. Similarly,  $P^-$  is related to the potential interaction energy between the quark and the antiquark (again in their rest frame) through the relation [13]

$$V(x_L, x_\perp) = P^- v^+, \quad (3.4)$$

i.e., for zero transverse separation one obtains

$$V(x_L, 0) = G^2 \frac{\pi}{2} |x_L|. \quad (3.5)$$

As soon as the  $Q\bar{Q}$  pair is separated by at least one transverse site, the result is less trivial. For example, when the transverse separation is one lattice spacing, one obtains an integral equation for the wave function of the (one) gluon connecting the  $Q\bar{Q}$  pair

$$\begin{aligned} P^- \psi(k^+) &= \left( \frac{k^+}{2v^{+2}} + \frac{m^2}{2k^+} \right) \psi(k^+) + G^2 \int_0^\infty dq^+ \\ &\quad \times \frac{(q^+ + k^+) [\psi(k^+) - \psi(q^+) e^{i(k^+ - q^+)x^-/2}]}{2\sqrt{k^+ q^+} (q^+ - k^+)^2} \\ &\quad + G^2 \int_0^\infty dq^+ \\ &\quad \times \frac{(q^+ + k^+) [\psi(k^+) - \psi(q^+) e^{i(q^+ - k^+)x^-/2}]}{2\sqrt{k^+ q^+} (q^+ - k^+)^2}, \end{aligned} \quad (3.6)$$

where the two interaction terms arise from the Coulomb coupling of the gluon to the quark and antiquark, respectively. Equations (3.3) and (3.4) also hold here. The exponential ‘‘form factors’’ in the interaction terms arise since the quark and antiquark are displaced in the longitudinal direction. The coefficient  $m^2$  is proportional to  $c_2$  in the normal ordered effective potential. We renamed it because in Eq. (3.6) its physical meaning as an effective mass for the link field becomes apparent.

In the continuum (i.e., when one solves this integral equation exactly) the resulting  $V(x_L, x_\perp)$  is independent of the velocity  $v^+$ . Note that this is not the case when one uses DLCQ to solve the integral equation. This point will be discussed below.

For a separation of two sites the integral equation for the two gluons between the charges reads

$$\begin{aligned} P^- \psi(k_1^+, k_2^+) &= \left( \frac{k_1^+ + k_2^+}{2v^{+2}} + \frac{m^2}{2k_1^+} + \frac{m^2}{2k_2^+} \right) \psi(k_1^+, k_2^+) + G^2 \int_0^\infty dq^+ \frac{(q^+ + k_1^+) [\psi(k_1^+, k_2^+) - \psi(q^+, k_2^+) e^{i(k_1^+ - q^+)x^-/2}]}{2\sqrt{k_1^+ q^+} (q^+ - k_1^+)^2} \\ &\quad + G^2 \int_0^\infty dq^+ \frac{(q^+ + k_2^+) [\psi(k_1^+, k_2^+) - \psi(k_1^+, q^+) e^{i(q^+ - k_2^+)x^-/2}]}{2\sqrt{k_2^+ q^+} (q^+ - k_2^+)^2} \\ &\quad + G^2 \int_0^{k_1^+ + k_2^+} dq^+ \frac{(q^+ + k_1^+) (k_1^+ + 2k_2^+ - q^+) [\psi(k_1^+, k_2^+) - \psi(q^+, k_2^+)]}{4\sqrt{k_1^+ k_2^+} q^+ (k_1^+ + k_2^+ - q^+)} \frac{1}{(q^+ - k_1^+)^2} + G^2 \frac{\pi}{4\sqrt{k_1 k_2}} \psi(k_1^+, k_2^+). \end{aligned} \quad (3.7)$$

The three interaction terms in Eq. (3.7) arise from the interaction of the first gluon with the quark, the second gluon with the antiquark, and the interaction between the two gluons, respectively.

The generalization of these expressions to more than two links is straightforward but the resulting expressions are very lengthy and will be omitted here.

Note that we used the ‘‘Coulomb trick’’ [25] in Eqs. (3.6) and (3.7) by adding and subtracting analytically a term in the interaction. This results in an interaction that vanishes for constant wave functions—which is close to the actual shape—and thus numerical convergence is improved considerably:

$$\int_0^1 \frac{dy}{(x-y)^2} \left\{ \frac{(x+y)(2-x-y)}{\sqrt{xy(1-x)(1-y)}} \psi(y) - 4\psi(x) \right\} = \int_0^1 \frac{dy}{(x-y)^2} \left\{ \frac{(x+y)(2-x-y)}{\sqrt{xy(1-x)(1-y)}} [\psi(y) - \psi(x)] \right\} - \frac{\pi\psi(x)}{\sqrt{x(1-x)}} + \frac{4\psi(x)}{x(1-x)}, \quad (3.8)$$

as well as

$$\int_0^\infty \frac{dy}{(x-y)^2} \left\{ \frac{(x+y)}{\sqrt{xy}} \psi(y) - 2\psi(x) \right\} = \int_0^\infty \frac{dy}{(x-y)^2} \left\{ \frac{(x+y)}{\sqrt{xy}} [\psi(y) - \psi(x)] \right\} + \frac{2\psi(x)}{x}, \quad (3.9)$$

Even though these integral equations will be solved below in their fully relativistic form, it is very instructive to consider various approximations thereof—particularly the limit  $m^2 \rightarrow \infty$ . Making a nonrelativistic expansion around the minimum of the kinetic terms one finds, for the (rest frame) potential energy for an arbitrary configuration with gluon (rest frame) positions at  $x_1, \dots, x_{n_\perp}$ ,

$$V = n_\perp m + G^2 \frac{\pi}{2} \left[ \left| -\frac{x_L}{2} - x_1 \right| + \left| x_{n_\perp} - \frac{x_L}{2} \right| + \sum_{i=1}^{n_\perp-1} |x_i - x_{i+1}| \right]. \quad (3.10)$$

Clearly, this expression is minimized for  $-x_L/2 < x_1 < \dots < x_{n_\perp} < x_L/2$  with a minimum value

$$V(x_L, x_\perp) = n_\perp m + G^2 \frac{\pi}{2} |x_L|. \quad (3.11)$$

For large  $m$  this is the  $Q\bar{Q}$  potential in the rest frame of the pair, which thus exhibits linear confinement [13]. Since the lattice spacing has not yet been fixed, we are free to choose

$$a = \frac{2m}{\pi G^2}, \quad (3.12)$$

which renders the longitudinal and the transverse string tension equal to each other. Nevertheless,  $V$  in Eq. (3.11) is still not rotationally invariant: for example, for  $x_L = x_\perp = x$  one finds  $V(x, x) = 2V(0, x)$ . For a rotationally invariant linear potential the result would have been  $V(x, x) = \sqrt{2}V(0, x)$ .

Such a result is familiar from the strong coupling limit in Euclidean or Hamiltonian lattice QCD, where one obtains exactly the same square shaped equipotential lines. Of course, once one no longer restricts oneself to the strong coupling limit, the quantum mechanical fluctuations tend to restore rotational invariance.

This is also what happens here. To see this, let us consider a  $Q\bar{Q}$  pair separated by one transverse lattice unit. When the (rest frame) positions of the quark and the antiquark are both at  $x_L = 0$  then the gluon in between them experiences a potential energy equal to

$$V_{\text{aligned}}(x_1) = G^2 \pi |x_1|. \quad (3.13)$$

In contrast, when the positions of the quark and the antiquark are at  $\pm x_L/2 \neq 0$  the potential energy which the gluon in between them experiences is

$$V_{\text{displaced}}(x_1) = \frac{G^2 \pi}{2} \left[ \left| -\frac{x_L}{2} - x_1 \right| + \left| \frac{x_L}{2} - x_1 \right| \right] = \begin{cases} G^2 \pi |x_1| & \text{for } |x_1| > \frac{|x_L|}{2}, \\ G^2 \pi \frac{|x_L|}{2} & \text{for } |x_1| < \frac{|x_L|}{2}. \end{cases} \quad (3.14)$$

The violation of rotational invariance in the large  $m$  limit manifests itself through the fact that the minimum of the potential (with respect to  $x_1$ ) for the displaced case is too high compared to the aligned case.

The crucial point is (see Fig. 2) that the valley of the potential in the displaced case [Eq. (3.14)] is wider than the valley of the potential in the aligned case [Eq. (3.13)]. Therefore, corrections due to the quantum mechanical zero-point energy tend to increase the energy more strongly in the aligned case than in the displaced case. In a sense, quantum mechanical corrections work in the right direction to help restore rotational invariance.

Even though this simple quantum mechanical argument is very useful in order to understand the physics of the restoration of rotational invariance, we will not attempt to make it quantitative since we will now make a fully relativistic calculation, where we actually solve light-front integral equations for these systems, Eqs. (3.6), (3.7), and the generalization to more sites.

As we have seen above, the mass term plays an important role in setting the scale for the transverse string tension. In fact, given the string tension  $\sigma$ , one obtains  $a = m/\sigma$  for large  $m^2$ . Thus, if one wants to be close to the continuum limit, one should try to make  $m^2$  as small as possible. It turns out that below  $m^2 = 0$ , the spectrum becomes tachyonic [23], i.e.,  $m^2 = 0$  is the smallest meaningful value. As we will see below, the string tension in lattice units (i.e., also the lattice spacing in physical units) remains finite at  $m^2 = 0$ . Since  $m^2 = 0$  is thus the closest we can get to the continuum limit within our approximation, we will focus only on this value. We should also emphasize at this point that while smaller values of  $m$  imply smaller lattice spacings, it will not be sufficient to just make  $a$  small enough in order to reach the continuum limit. Simultaneously, one will have to determine the higher order terms in the effective potential as we discussed above. Nevertheless it is true that, for a given effective

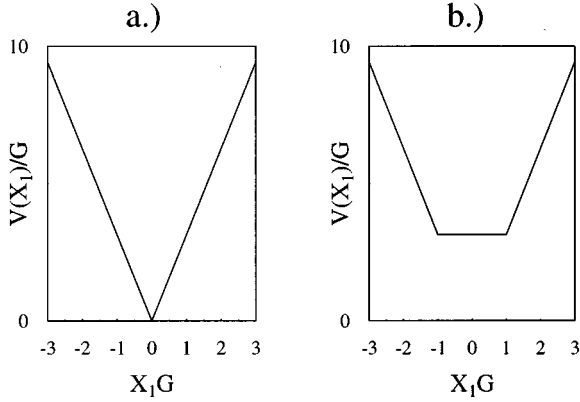


FIG. 2. Potential energy of a gluon between an external  $Q\bar{Q}$  pair separated by one link in the (fictitious) nonrelativistic limit: (a) for  $Q$  and  $\bar{Q}$  at the same longitudinal position, (b) for  $Q$  and  $\bar{Q}$  displaced in the longitudinal direction by  $x_L = 2/G$ .

tive potential, decreasing the mass term corresponds to smaller lattice spacings so that it is in general desirable to work with a small mass term.

In order to fix the scales, we first determine the transverse string tension. There are two possibilities to determine this observable. One is to consider the  $Q\bar{Q}$  potential for large separations of the pair. The other is to consider a torus geometry, where the energy of glueball states which “wrap around” the torus is equal to the string tension times the circumference of the circle [24]. Even though the latter method cannot be used to calculate the  $Q\bar{Q}$  potential or to calculate the string tension in any direction other than the transverse direction, it turns out to converge faster than calculations of the  $Q\bar{Q}$  potential. Therefore, “wrap-around glueballs” were used to fix the string tension in this work.

In the calculation of the glueball masses, we used DLCQ [14] with antiperiodic boundary conditions, because the convergence in the DLCQ parameter  $K$  is faster than with periodic boundary conditions. Finally, the masses of “wrap-around glueballs” were calculated for a fixed size of the periodic lattice as a function of the DLCQ parameter  $K$  and the results were extrapolated to  $K \rightarrow \infty$  (Fig. 3).

The transverse string tension (in lattice) was then extracted by considering the resulting extrapolated masses of these states as a function of the number of lattice spacings. Note that, as the nearly equidistant spacing in Fig. 3 indicates, already for only a few lattice spacings, the mass of these states depends almost exactly linearly on the number of transverse lattice spacings, which allows one to easily extract the transverse string tension from these data. The fitted result is

$$\frac{M(n)}{G} \underset{n \rightarrow \infty}{\sim} n \sigma_{\perp} a \approx n(1.30 \pm 0.03), \quad (3.15)$$

where we introduced the transverse string tension and the transverse lattice spacing. If one denotes the longitudinal string tension by  $\sigma_L$ , one finds [Eq. (3.5)]

$$\sigma_L = G^2 \frac{\pi}{2} \quad (3.16)$$

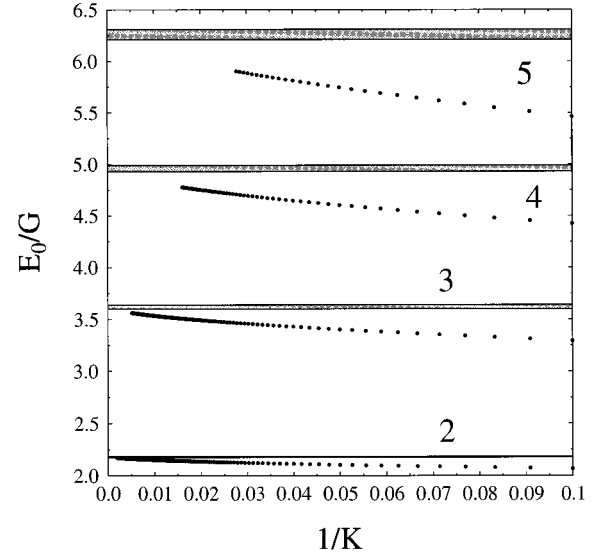


FIG. 3. Ground state energy of winding modes for several transverse sizes  $n_{\perp}$  of the lattice as a function of the inverse DLCQ parameter  $K$ . The shaded bands correspond to the  $K \rightarrow \infty$  extrapolated results for the ground state energies. The width of the bands reflects systematic uncertainties in the extrapolation.

and if one furthermore imposes  $\sigma_L = \sigma_{\perp} = \sigma$  one finds for the transverse lattice spacing in physical units

$$a \stackrel{\text{def}}{=} \frac{\lim_{n \rightarrow \infty} [M(n)/n]}{\sigma_{\perp}} \approx \frac{1}{G} (0.83 \pm 0.02). \quad (3.17)$$

Having related the longitudinal and transverse scales, we are now in a position to explore the  $Q\bar{Q}$  potential. Note that even though the “wrap-around glueballs” are quite useful in the determination of the purely transverse string tension, they cannot be used to determine the string tension for any direction other than the transverse direction and they also cannot be used to determine the  $Q\bar{Q}$  potential for finite separations. The  $Q\bar{Q}$  potential will therefore be determined by using the fixed charges formalism outlined above. Nevertheless, since—as we will see below—the determination of the string tension from the  $Q\bar{Q}$  potential through the fixed charges formalism is less accurate than the method using wrap-around glueballs, we will still use the latter method to fix the scales in the following calculation.

In the calculation of the  $Q\bar{Q}$  potential we proceeded as follows: For a given longitudinal separation  $x^-$  and a given velocity  $v^+$ , the DLCQ Hamiltonian (for a given number of transverse sites) was constructed with a cutoff on the total longitudinal momentum of the gluon string.<sup>3</sup> Since the momenta are discrete,  $v^+$  provides an infrared cutoff in the following sense: the peak of the wave function, will be at momenta of order  $k^+ \approx v^+ G$ . That is, only if  $v^+ G$  is large in

<sup>3</sup>In contrast to DLCQ calculations of glueball masses, the momentum is not conserved here since arbitrary momenta can be transferred to and from the external charges.

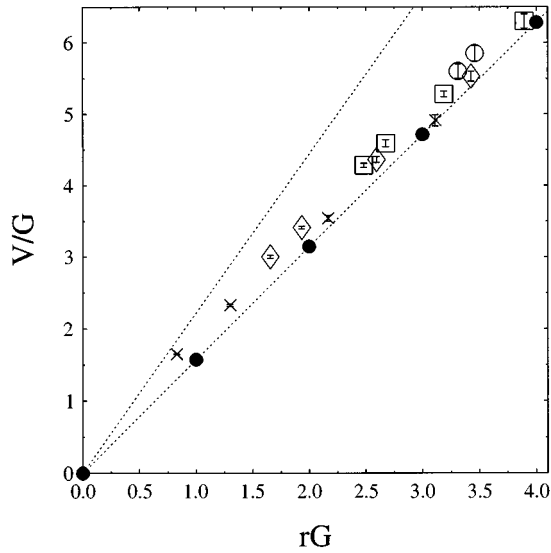


FIG. 4.  $Q\bar{Q}$  potential vs  $r$ , where  $r^2 = x_\perp^2 + x_L^2$ , as extracted from the light-front Hamiltonian in the approximation where only one gluon per link is allowed. The error bars reflect the uncertainties arising from the extrapolation to the continuum limit in the DLCQ calculation. The transverse scale was fixed from the masses of “wrap-around glueballs.” The fact that not all points lie on the same smooth curve reflects the residual anisotropy due to the Fock space truncation and the use of an oversimplified effective potential. For comparison, the two dashed lines give the range of values one would obtain in the large  $m$  limit,  $V \propto |x_L| + |x_\perp|$ . Dots, crosses, diamonds, squares, and circles correspond to  $n_\perp = 0, 1, 2, 3, 4$ , respectively.

integer units, one will not be affected by the cutoff. Thus one must perform a careful extrapolation,<sup>4</sup> where one sends both the UV cutoff, but also the velocity  $v^+$  to infinity. The actual numerical work was based on DLCQ with antiperiodic boundary conditions on the link fields. The ground state energies and wave functions for the resulting DLCQ Hamiltonians were determined using a Lanczos algorithm [26]. The resulting  $Q\bar{Q}$  potential is shown in Fig. 4.

Even though not all points on Fig. 4 lie on the same smooth curve, there is still a significant improvement compared to the large  $m$  limit (3.11), where values for  $V(x_L, x_\perp)$  would fill the whole area within the two dashed lines in Fig. 4. The residual anisotropy is mostly due to the use of an oversimplified effective potential [Eq. (2.4)] but also due to the (*ad hoc*) suppression of higher Fock components (see also the results below obtained without Fock space truncation). Nevertheless, the restoration of rotational invariance is quite impressive as a contour plot for the same data as in Fig. 4 shows (Fig. 5).

The lines of the constant potential turn out to be almost circles. The slight anisotropy of the data in Fig. 4 results in a slight ellipsoidal distortion in Fig. 5. Note that the ellipsoidal shape in Fig. 5 does *not* mean that the string tension in the longitudinal and transverse directions are different. In fact they are the same by construction, i.e., by the choice for the

<sup>4</sup>This must be done very carefully because the peak of the wave function moves as one changes  $v^+$ .

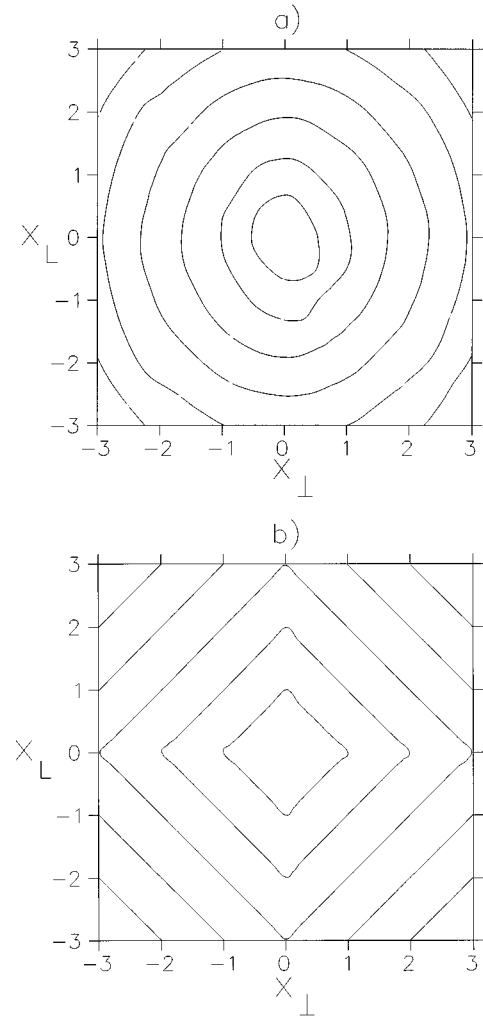


FIG. 5. (a) Contour plot for the  $Q\bar{Q}$  potential vs  $x_\perp$  and  $x_L$  in the approximation where we keep only one gluon per link. For comparison, the contour plot for the  $Q\bar{Q}$  potential in the large  $m$  (strong coupling) limit ( $V \propto |x_L| + |x_\perp|$ ) is shown in (b).

lattice unit. What is going on here is that, while  $V(x_L, 0) = G^2(\pi/2)|x_L|$  in the approximation chosen in this work, the potential in the transverse direction satisfies  $V(0, x_\perp) \xrightarrow{x_\perp \rightarrow \infty} G^2(\pi/2)|x_\perp| + c$ , which has the same string tension in the longitudinal and transverse direction but which results in equipotential lines that look like ellipses.

#### IV. THE MOMENTUM CARRIED BY THE GLUE

Even though the calculations presented in this paper are still very crude, the approximate rotational invariance of the  $Q\bar{Q}$  potential is very encouraging so that we proceed to investigate other physical observables. We picked the gluon distribution in these  $Q\bar{Q}$  systems since one of the main motivations to study light-front QCD in the first place is the direct access to parton distributions measured in deep inelastic scattering. In particular, we will focus on the (light-front) momentum carried by the gluon component.

Before we proceed, we should caution the reader that the results must be interpreted with care: Since we work with

finite and large lattice spacing, the ‘‘gluons’’ are not point-like ‘‘current gluons’’ and thus the distribution functions should be considered as distribution functions of some kind of ‘‘constituent gluons.’’ Nevertheless, the results might be helpful in obtaining some intuitive insight about the parton structure at low  $Q^2$ .

Obviously, when the external charges are sitting on the same site, there are no gluons within the approximation considered in this paper and thus the gluons carry zero momentum for such a configuration. The other extreme is when the charges are separated only transversely, in which case one can derive an exact result.

Consider Eq. (3.6) for  $x^- = 0$ :

$$\begin{aligned}
 P^- \psi(k^+) &= \left( \frac{k^+}{2v^{+2}} + \frac{m^2}{2k^+} \right) \psi(k^+) \\
 &+ G^2 \int_0^\infty dq^+ \frac{(q^+ + k^+) [\psi(k^+) - \psi(q^+)]}{2\sqrt{k^+ q^+} (q^+ - k^+)^2} \\
 &+ G^2 \int_0^\infty dq^+ \frac{(q^+ + k^+) [\psi(k^+) - \psi(q^+)]}{2\sqrt{k^+ q^+} (q^+ - k^+)^2}.
 \end{aligned} \tag{4.1}$$

On the one hand (see Appendix A) one knows that

$$P^- = \frac{\langle V \rangle}{v^+}, \tag{4.2}$$

where  $\langle V \rangle$  is the expectation value for potential (rest-frame) energy in this configuration. On the other hand, from the Feynman-Hellman theorem for variations of  $P^-$  with respect to  $v^+$  in Eq. (4.1) one finds

$$\frac{d}{dv^+} P^- = - \frac{1}{v^{+3}} \int_0^\infty dk^+ |\psi(k^+)|^2 k^+. \tag{4.3}$$

Combining these two results, one thus finds the remarkably simple result (valid for  $Q\bar{Q}$  pairs that are separated only transversely)

$$P_{\text{glue}}^+ \equiv \int_0^\infty dk^+ |\psi(k^+)|^2 k^+ = \langle V \rangle v^+ \tag{4.4}$$

which states that the momentum carried by the gluons is proportional to the energy in the gluon field. Applying the same reasoning to Eq. (3.7) (again for  $x^- = 0$ ), one obtains similarly

$$P_{\text{glue}}^+ \equiv \int_0^\infty dk_1^+ dk_2^+ |\psi(k_1^+, k_2^+)|^2 (k_1^+ + k_2^+) = \langle V \rangle v^+, \tag{4.5}$$

which has the same simple interpretation as Eq. (4.4). The generalization to more than two links is straightforward and obvious:

$$\begin{aligned}
 P_{\text{glue}}^+ &\equiv \int_0^\infty dk_1^+ \cdots dk_n^+ |\psi(k_1^+, \dots, k_n^+)|^2 (k_1^+ + \cdots + k_n^+) \\
 &= \langle V \rangle v^+.
 \end{aligned} \tag{4.6}$$

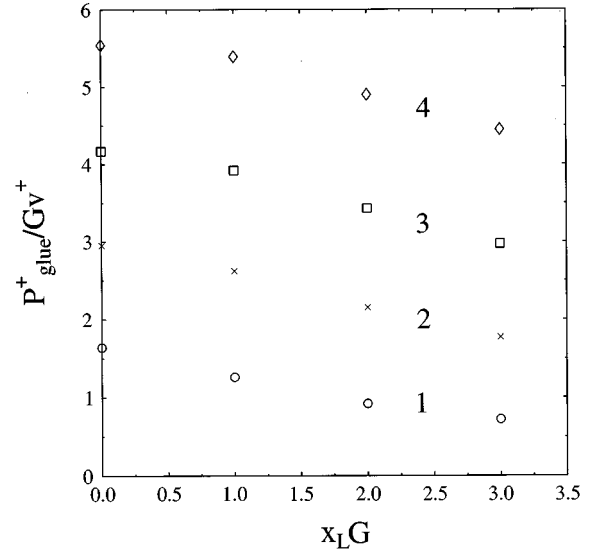


FIG. 6. Momentum carried by the gluons for external charges that are separated by  $n_\perp = 1, \dots, 4$  lattice spacings as a function of the longitudinal (rest-frame) separation of the external charges. The results are obtained in the one-gluon-per-link approximation. For  $n_\perp = 0$  the gluons carry no momentum in this approximation.

Note that similar sum rules have been derived elsewhere [27] and they are not limited to the Fock space truncated version.

In the general case, where both  $x_L$  and  $x_\perp$  are nonzero, we were not able to find a generalization of Eq. (4.6). However, we can easily use the numerically obtained states from the calculation of the ground state energy and just ‘‘measure’’ the momentum carried by the glue. The result is shown in Fig. 6.

First of all, one notices that the momentum carried by the gluons increases as the transverse separation increases. This result is intuitively obvious and happens for  $x_L = 0$  in a way that is consistent with Eq. (4.6). A much less obvious result is that, for fixed  $n_\perp$ , the momentum carried by the gluons *decreases* for increasing longitudinal separation. This result is at first counterintuitive because the energy in the gluon field increases when one increases  $x_L$  for fixed  $n_\perp$ . However, this apparent paradox gets resolved when one recalls that only transverse components of the electric field contribute to the momentum of the state in the infinite momentum frame [28]. Assuming (for simplicity) that the  $Q\bar{Q}$  pair is connected by a straight gluon string, it is obvious that the transverse component decreases as the string gets rotated into the longitudinal direction. This also explains why the momentum carried by the gluons depends not only on the separation of the  $Q\bar{Q}$  pair but also on its orientation. As an idealized case, it is instructive to assume that the  $Q\bar{Q}$  pair is connected by a straight string, i.e., the electric field lines are parallel to the  $Q\bar{Q}$  axis (which has an angle with the longitudinal direction that we will denote by  $\Theta$ ). If  $|\vec{E}_\perp|$  is the field strength in the string then  $|\vec{E}_\perp| = |\vec{E}| \sin\Theta$ . In Ref. [28] it has been shown that the momentum carried by the gauge bosons is proportional to the volume integral of  $\vec{E}_\perp^2$  i.e., one would expect

$$P_{\text{glue}}^+/v^+ \propto r \sin^2 \Theta = x_{\perp} \sin \Theta = \frac{x_{\perp}^2}{\sqrt{x_{\perp}^2 + x_L^2}}, \quad (4.7)$$

which qualitatively explains the decrease of  $P_{\text{glue}}^+$  for fixed  $x_{\perp}$  with increasing  $x_L$ .

The qualitative conclusion that one can take from these results is that for heavy  $Q\bar{Q}$  systems, such as  $J/\psi$  or  $\psi$  mesons, it is quite natural that the gluons carry a fraction

$$x_{\text{glue}} \equiv \frac{P_{\text{glue}}^+}{P_{\text{total}}^+} = c \frac{\langle V \rangle}{M_{Q\bar{Q}}} \quad (4.8)$$

of a hadron's momentum, where  $c$  is a ‘‘geometry factor,’’ which is of the order 1.

## V. INCLUDING HIGHER FOCK COMPONENTS

Even though the results in Sec. III are already amazingly close to being rotationally invariant, they have a serious flaw: they were obtained after an *ad hoc* truncation of the Fock space to the minimal component ( $\leq 1$  quanta per link). While this provided us with a very intuitive and numerically acceptable ‘‘quantum mechanical’’ approach to the gluon distribution, it gives rise to results that are still very close to the strong coupling limit: in fact, even though the fields may fluctuate longitudinally (which distinguishes the above valence approximation from the strict strong coupling limit) QED and QCD still give identical static potentials at this level. One might thus be sceptical about the results obtained—especially about the linearly rising  $Q\bar{Q}$  potential. In this section, we will provide evidence that the results obtained for the  $Q\bar{Q}$  potential do *not* depend very much on the valence approximation.

The main difference between the results in this section and the results in the previous section is that we allowed for one additional link-antlink pair in the string state. Computer storage and the algorithm that we were using (Lanzcos, where we stored all nonzero matrix elements and their addresses in order to keep the code fast) did not allow us to go beyond one additional pair while at the same time being able to extrapolate to the continuum limit for two or more links. However, our calculations with one additional pair showed that this component of the wave function is already very strongly suppressed compared to the valence component so that we do not expect significant changes of the result by going to even higher Fock components. Also, we should point out that with just one additional pair there is a difference between QED and QCD.

The effective potential was taken to be the same as the one we used for the valence calculation, namely just a quadratic term and we did the calculations with the ‘‘mass’’ at the first-order critical point. We should emphasize that adding higher order terms to the effective potential only affects the calculation through higher Fock components. Therefore (unless the coefficients of the higher order terms are taken to be very large to invalidate the perturbative argument) we expect the  $Q\bar{Q}$  potential to be rather insensitive to such higher order terms. This is in sharp contrast to glueball calculations where even the ground state spectrum depends strongly on the higher order terms [24]. The rest of the cal-

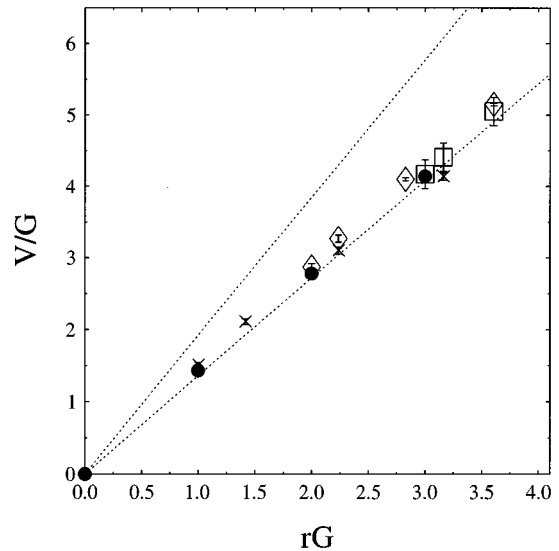


FIG. 7. Contour plot for the  $Q\bar{Q}$  potential vs  $x_{\perp}$  and  $x_L$  in the approximation where we allow for up to one additional link-antlink pair.

culational procedure strongly resembled the calculation in the previous section. Because of limitations of our algorithm, we had to restrict ourselves to three or less lattice sites.

The most important result was that higher Fock components in the ground state of the string had a norm of typically only a few percent, with the resulting energy shifts slightly larger but still of the same order of magnitude. In fact, this justifies the truncation to only one pair. The results for the  $Q\bar{Q}$  potential and the momentum carried by the glue are shown in Figs. 7 and 8, respectively.

The first thing that one notes when one compares Fig. 4 and Fig. 7 is an increase in the size of the error bars. This is because we had to limit ourselves to smaller values of the longitudinal momentum and the systematic uncertainties from the extrapolation increased. Another obvious observation is that by including an additional pair the result gets even closer to being rotationally invariant. We find that very encouraging for future calculations. Apart from that, the only difference between the calculations with and without the extra pair is a renormalization of the string tension in lattice units [ $a_{\perp} = 1.14\sigma^{-1/2}$  compared to  $a_{\perp}(\text{valence}) = 1.04\sigma^{-1/2}$ ].

The momentum carried by the glue no longer has to vanish for a  $Q\bar{Q}$  pair that is oriented longitudinally (Fig. 8). Nevertheless, the numerical result is very small, which reflects the small admixture from higher Fock components. In fact, similar to the potential, there is only very little change for the momentum carried by the glue when one compares calculations with (Fig. 8) and without (Fig. 6) link-antlink pairs.

Overall, we found only a small change in the results for the ground state of the string as we allowed for higher Fock components. We find this a very encouraging result since it may allow one to construct models for quarkonia that have a similar truncation in the Fock space.

## VI. SUMMARY AND OUTLOOK

We have presented analytical and numerical calculations for the rest-frame  $Q\bar{Q}$  potential in QCD on a transverse lat-



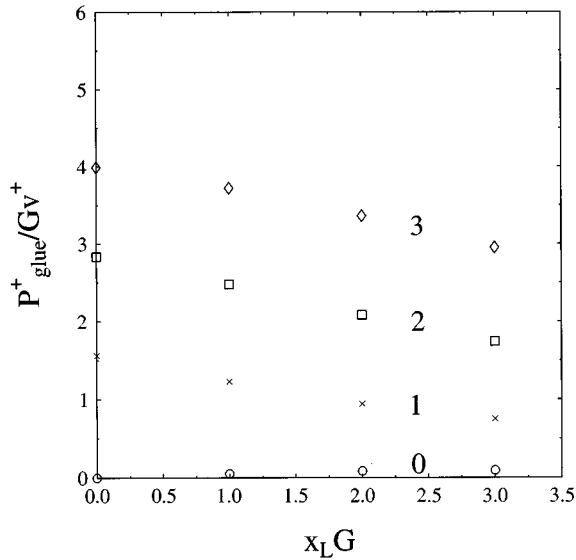


FIG. 8. Momentum carried by the gluons for external charges that are separated by  $n_{\perp} = 0, \dots, 3$  lattice spacings as a function of the longitudinal (rest-frame) separation of the external charges. The results are obtained in the one-gluon-per-link approximation plus one additional pair.

tice using light-front quantization. The rest-frame  $Q\bar{Q}$  potential was obtained by considering the invariant mass of a heavy  $Q\bar{Q}$  pair that moves with constant velocity and fixed separation.

First we showed analytically, that one obtains a linear potential (both in the longitudinal as well as in the transverse direction) in the limit of large transverse lattice spacings. This limit is similar to the strong coupling limit in Hamiltonian or Euclidean lattice QCD. The confinement mechanism for QCD in LF gauge in this limit depends on the orientation of the external charges: In the longitudinal direction, confinement arises from the instantaneous interaction which appears when the unphysical component of the gluon field is eliminated by solving the LF gauge analog of the Poisson equation. This component of the gluon field is also unphysical in the sense that it carries no momentum in the infinite momentum frame. Thus, for a purely longitudinally separated  $Q\bar{Q}$  pair the gluon field carries no momentum at all in the limit of large transverse lattice spacings—even though there is potential energy in the gluon field. For transversely separated charges, a completely different confinement mechanism is at work for large transverse lattice spacings: gauge invariance demands that the  $Q\bar{Q}$  pair is connected by a string of gauge-link field.<sup>5</sup> The “strong coupling limit” in Hamiltonian QCD corresponds on a transverse lattice to the limit, where the Lagrangian for the gluon link contains a large mass and thus the ground state energy of a gluon configuration is obtained by counting links. Together with the instantaneous interaction between quarks and adjacent link fields as well as among adjacent link fields, one thus obtains a square shaped linear potential—a result that is

<sup>5</sup>Even if one is not dogmatic about gauge invariance, infrared divergences, that occur otherwise, practically enforce this condition.

familiar from the strong coupling limit. Note that the link fields carry momentum in the infinite momentum frame, i.e., for transversely separated  $Q\bar{Q}$  pairs, the gluons do carry a sizable fraction of the total momentum.

Even though such an extreme asymmetry—no momentum carried by the gluons for purely longitudinal separations—is the result of the strong coupling limit, it is actually quite natural and physical that there is such an asymmetry depending on the orientation. This effect occurs already in QED [28] and arises from the fact that the component of the (color) electric which is transverse to the boost direction transforms differently from the component parallel to it. In particular, the parallel component does not contribute to the Pointing vector in the infinite momentum frame. For this reason, and because of the difference in the field distribution between QED and QCD (dipole versus string) we expect a stronger orientational dependence of the gluon momentum in QCD than in QED.

In the next step we performed numerical calculations of the  $Q\bar{Q}$  potential. First we showed results where we truncated the Fock space to not more than one quantum of the link field for each transverse link. Otherwise, the link fields were treated fully dynamical and were allowed to move freely in the longitudinal direction. There was only a first-order transition as a function of the link field mass, i.e., while the transverse lattice spacing in physical units decreased with the mass term, it did not approach zero at the critical point. Nevertheless, the numerically obtained  $Q\bar{Q}$  potential at the critical point was almost rotationally invariant. The reason for the first-order critical point was most likely our oversimplified choice of the effective link field potential  $V_{\text{eff}}(U)$ .

Even though the numerical precision was only limited, we then showed that the qualitative results change only little when we allowed for excited Fock space components. This is very important, since only upon inclusion of higher Fock components is there a difference between QED and QCD. The unimportance of higher Fock components in the ground state of the string is presumably partly responsible for the approximate rotational invariance of our results. The reason is that in general one would not expect rotational invariance on a coarse lattice unless one includes the full effective potential for the link fields — from which we kept only the quadratic term. Those terms that we omitted contribute only to matrix elements that include higher Fock components. Therefore, if higher Fock components are not important for the  $Q\bar{Q}$  potential then the higher order terms in  $V_{\text{eff}}(U)$  cannot be important either.<sup>6</sup> For tests of rotational invariance that are sensitive to the higher order terms in  $V_{\text{eff}}(U)$  one must therefore study other observables, such as glueball spectra [24].

The numerical results, both with and without truncation of the Fock space, confirmed the strong dependence of the momentum carried by the glue on the orientation of the external

<sup>6</sup>Note that this argument is not fully complete since we have not verified that the higher Fock components are unimportant for the ground state of the string after the higher order terms are included in  $V_{\text{eff}}(U)$ .

pair. This might have observable consequences for heavy quarkonia with nonzero orbital angular momentum.

There are many extensions of this work that one could think of, such as studying excited states of the string or using Monte Carlo algorithms for obtaining the eigenstates and eigenvalues of the LF Hamiltonian. Excited states would be interesting both for theoretical but also for phenomenological reasons. On the theoretical side, since higher Fock components play a stronger role in the excited states of the string, they would allow probing the relevance of the higher order terms in  $V_{\text{eff}}(U)$  for rotational invariance and could thus be used to help fix those constants. From the phenomenological point of view, the excited states of the string are interesting because of their connection to hybrid states. Employing Monte Carlo algorithms [30] when studying the transverse lattice might be a useful option since that would allow one to include many more Fock components than otherwise. Repeating the calculations in 3+1 dimensions is an obvious extension of this work [31]. One possibility in this direction, which we are currently exploring, is to repeat the minimal Fock space truncation and to fit the plaquette interaction term such that approximate rotational invariance in all 3 spatial directions is achieved. Then one can use this gluonic interaction to investigate the physics of the ground and excited states of heavy quarkonia.

#### ACKNOWLEDGMENTS

M.B. acknowledges useful discussions with F. Antonuccio, S. Dalley, H. J. Pirner, and B. van de Sande. This work was supported by the D.O.E. under Contract No. DE-FG03-96ER40965 and in part by TJNAF.

#### APPENDIX A: HOW TO MEASURE THE REST-FRAME $Q\bar{Q}$ POTENTIAL IN A LIGHT-FRONT CALCULATION

In this appendix,<sup>7</sup> a scheme is developed which allows one to extract the  $Q\bar{Q}$  potential, i.e., the quantity which corresponds to the potential between two infinitely heavy quarks in a rest frame, from a light-front calculation.<sup>8</sup> There are several reasons to study this observable in the light-front (LF) framework.

The LF formalism lacks manifest rotational invariance. Therefore, if one starts with a *wrong* LF Hamiltonian for QCD, the result  $V(\vec{R})$  depends on the orientation of  $\vec{R}$  with respect to the three-axis.<sup>9</sup> A measurement of  $V(\vec{R})$  thus provides a direct probe of rotational invariance in a physical observable.

This sensitivity of  $V(\vec{R})$  to rotational symmetry can then be exploited in the renormalization procedure to help determine noncovariant counter terms.

And, most importantly,  $V(\vec{R})$  in QCD is very well known over a large range of distances from the spectroscopy of

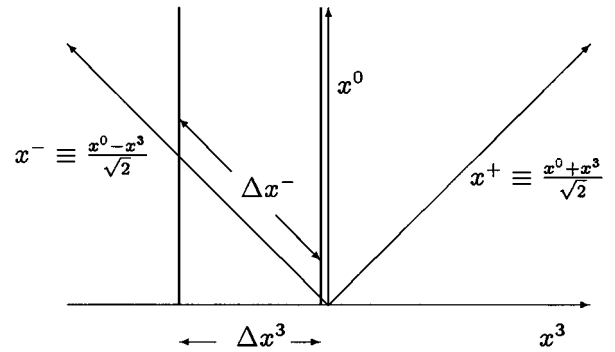


FIG. 9. World lines for two charges with longitudinal separation  $\Delta x^3$  in the rest frame.

heavy  $Q\bar{Q}$  mesons as well as from nonperturbative Euclidean lattice calculations (at least in the absence of dynamical quarks—but it is easy to make the same approximation in a LF framework).

Before we embark on deriving the effective LF Hamiltonian for two infinitely heavy sources, it is instructive to understand physically what it means to have two fixed sources “at rest”<sup>10</sup> from the LF point of view. As should be clear from Fig. 9, *fixed charges* in a *conventional frame* correspond to *charges that move with constant velocity* on the LF ( $v^+ = v^- = 1/\sqrt{2}$  in the example in Fig. 9). Furthermore, if the longitudinal separation is  $\Delta x^3$  in the rest frame, the charges have fixed separation  $\Delta x^- = \sqrt{2}\Delta x^3$  in the longitudinal LF direction. In the more general case, where the charges are moving with constant four-velocity  $v^\mu$ , where  $\vec{v}_\perp = 0$  in the rest frame, one obtains  $\Delta x^- = \Delta x^3/v^+$ .

The transverse separation is the same on the LF as it is in a rest-frame description. Therefore, in order to understand the LF physics of charges that are fixed in a conventional frame with separation  $\vec{R} = (R^1, R^2, R^3)$ , we must first understand how to describe a “dumbbell,” with ends separated by  $(\Delta x^1, \Delta x^2, \Delta x^-) = (R^1, R^2, R^3/v^+)$ , that moves with constant velocity  $v^+$ .

#### 1. One heavy quark on the LF

A pair of sources, moving both with the same constant velocity  $v^\mu$ , can also be interpreted (and treated) as *one extended source* moving with constant velocity  $v^\mu$  (for simplicity, we will keep  $\vec{v}_\perp = \vec{0}$ ). This is reminiscent of heavy quarks and thus, as a warmup exercise, it is very instructive to consider one (pointlike) heavy quark on the LF first (see also Refs. [13,29]).

For simplicity, we will first take the heavy quark limit for the canonical Hamiltonian, which can be written in the form

$$P_B^- = \frac{M_b^2 + \vec{k}_{b\perp}^2}{2p_b^+} + P_{HL}^- + P_{LL}^-, \quad (\text{A1})$$

<sup>7</sup>See also Ref. [13].

<sup>8</sup>Even though the body of this paper is on (2+1)-dimensional QCD, we keep the discussion in this section independent of the number of transverse space-time dimensions.

<sup>9</sup>We use the notation  $A^\pm = A_\mp = (A^0 \pm A^3)/\sqrt{2}$ ,  $\vec{A}_\perp = (A^1, A^2)$ .

<sup>10</sup>Here we mean “at rest” for a conventional observer, i.e., in an equal time frame.

where  $B$  represents the hadron,  $b$  is the heavy quark,  $P_{HL}^-$  contains the interactions between heavy ( $b$ ) and light degrees of freedom, and  $P_{LL}^-$  contains all terms involving light degrees of freedom only. The heavy quark limit is obtained by making an expansion in inverse powers of the  $b$ -quark mass. For this purpose we write

$$p_b^+ = P_B^+ - p_L^+ = M_B v^+ - p_L^+, \quad (\text{A2})$$

where  $p_L^+$  is defined to be the sum of the longitudinal (LF) momenta of all light degrees of freedom. For the (total) LF energy we write on the LHS of Eq. (A1)

$$P_B^- = M_B v^- = \frac{M_B}{2v^+} = \frac{M_b + \delta E}{2v^+}, \quad (\text{A3})$$

where  $\delta E \equiv M_B - M_b$  is the ‘‘binding energy’’ of the hadron. After inserting Eqs. (A2) and (A3) into Eq. (A1) and expanding one obtains

$$\begin{aligned} \frac{M_b + \delta E}{2v^+} &= \frac{M_b^2 + \vec{k}_{b\perp}^2}{2(M_B v^+ - p_L^+)} + P_{HL}^- + P_{LL}^- \\ &= \frac{M_b^2 + \vec{k}_{b\perp}^2}{2(M_b v^+ + \delta E v^+ - p_L^+)} + P_{HL}^- + P_{LL}^- \\ &= \frac{M_b}{2v^+} - \frac{\delta E}{2v^+} + \frac{p_L^+}{2v^{+2}} + O\left(\frac{1}{M_b}\right) + P_{HL}^- + P_{LL}^-. \end{aligned} \quad (\text{A4})$$

Note that we have assumed that the transverse momentum of the heavy quark is small compared to its mass, which is justified in a frame where the transverse velocity of the heavy hadron vanishes. The term proportional to  $M_b$  cancels between the LHS and the RHS of Eq. (A4) and we are left with

$$\frac{\delta E}{v^+} = \frac{p_L^+}{2v^{+2}} + O(1/M_b) + P_{HL}^- + P_{LL}^-. \quad (\text{A5})$$

The *brown muck* Hamiltonian  $P_{LL}^-$  is the same as for light-light systems and will not be discussed here. The interaction term between the heavy quark and the brown muck ( $P_{HL}^-$ ) is more tedious but straightforward. For example, heavy quark pair creation terms (via instantaneous gluons) are proportional to  $1/(p_{b_1}^+ + p_{b_2}^+)^2 \propto 1/M_b^2$  and can thus be neglected. Similarly, pair creation of heavy quarks from virtual gluons is also suppressed by at least one power of  $M_b$ . This also justifies our omission of states containing more than one heavy quark from the start. Other terms that vanish in  $P_{HL}^-$  include interactions that involve *instantaneous exchanges* of heavy quarks, which are typically proportional to the inverse  $p^+$  of the exchanged quark and thus of the order  $O(M_b^{-1})$ . Up to this point, all interaction terms that we have considered vanish in the heavy quark limit. The more interesting ones are of course those terms which survive. The simplest ones are the instantaneous gluon exchange interactions with light quarks or gluons, which are, respectively,  $V_{Qq} \propto (p_q^+ - p_q'^+)^{-2}$  and  $V_{Qg} \propto (p_g^+ + p_g'^+)(p_g^+ - p_g'^+)^{-2}$  and remain unchanged in the limit  $M_b \rightarrow \infty$ . Terms which involve

instantaneous gluon exchange and are off diagonal in the brown muck Fock space behave in the same way.

The quark gluon vertex simplifies considerably. For finite quark mass one has for the matrix element for the emission of a gluon with momentum  $k$ , polarization  $i$ , and color  $a$  between quarks of momentum  $p_1$  and  $p_2$ :

$$P_{QQg}^- = -igT^a \left\{ 2 \frac{k^i}{k^+} - \frac{\vec{\sigma}_\perp \vec{p}_{2\perp} - iM_b}{p_2^+} \sigma^i - \sigma^i \frac{\vec{\sigma}_\perp \vec{p}_{1\perp} + iM_b}{p_1^+} \right\}, \quad (\text{A6})$$

where spinors as well as creation and/or destruction operators have been omitted for simplicity. In the heavy quark limit [note  $1/p_1^+ - 1/p_2^+ = O(M_b^{-2})$ ] the spin dependent terms drop out and one finds in the heavy quark limit

$$P_{QQg}^- = -2igT^a \frac{k^i}{k^+}. \quad (\text{A7})$$

The spin of the heavy quark thus decouples completely, giving rise to the well-known  $SU(2N_f)$  symmetry in heavy quark systems.

## APPENDIX B: TWO HEAVY SOURCES

As we discussed above, two heavy sources at fixed separation can formally be treated as one extended heavy source.<sup>11</sup> Therefore, the LF Hamiltonian for two sources is the same as for one source with two minor modifications.

All vertices involving a heavy source get modified according to the rule ( $\hat{O}$  stands for any operator acting on the brown muck)

$$\{\chi^\dagger T^a \chi \times \hat{O}\} + \text{H.c.}$$

$$\rightarrow \{[\chi_Q^\dagger T^a \chi_Q F_R(q) - \chi_{\bar{Q}}^\dagger T^a \chi_{\bar{Q}}' F_R(-q)] \times \hat{O}\} + \text{H.c.}, \quad (\text{B1})$$

where  $\chi$  stands for the operator acting on the color degrees of freedom of the heavy quark/antiquark. The ‘‘form factor’’

$$F_R(q) = \exp\left[\frac{i}{2} \left( \frac{q^+ R^3}{v^+} - \vec{R}_\perp \vec{q}_\perp \right)\right] \quad (\text{B2})$$

arises from acting with the (kinematic) displacement operator on the position of the heavy quark and/or antiquark (shifting it from  $x^- = 0$ ,  $\vec{x}_\perp = \vec{0}_\perp$  to  $x^- = \pm R^3/2v^+$ ,  $\vec{x}_\perp = \pm \vec{R}_\perp/2$ ) and  $q$  is the *net* momentum transferred to the brown muck. This rule holds irrespective of the number of gluons involved in this process. Note that  $\hat{O}$  (*brown muck*) is the same for one or two heavy sources.

There is a static potential between the two heavy quarks. In the continuum, the canonical Hamiltonian yields  $P_{HH}^- = g^2 \chi_Q^\dagger T^a \chi_Q \chi_{\bar{Q}}^\dagger T^a \chi_{\bar{Q}}' \delta^{(2)}(\vec{R}_\perp) |R^3| v^+$ . In general, there will be a more complicated dependence on  $\vec{R}$  which has to be determined by demanding self-consistency. For example, singularities arising from exchange of gluons with

<sup>11</sup>Just think of a dumbbell.

low  $q^+$  between the two sources should cancel (nonperturbatively) with the IR behavior of the instantaneous potential in  $P_{HH}^-$  [20].

Using Eq. (A5),  $V(\vec{R})$  can thus be extracted as follows:

(1) For a given  $\vec{R}$  and  $v^+$ , write down the effective LF Hamiltonian for the heavy pair interacting with the brown muck [including the form factors Eq. (B2) and including all the counterterms and counterterm functions which would also appear in a “heavy-light” system]. (2) The lowest eigenvalue  $\delta E^{(1)}$  from Eq. (A5), i.e., the QCD ground state in

the presence of the two heavy sources, is then equal to  $V(\vec{R})$ .

The heavy quark potential thus calculated is equivalent to the potential which a lattice theorist would extract from an asymmetric rectangular Wilson loop. Since there is plenty of “quenched” lattice data around, it would make sense to omit light quarks completely in a first approach and to focus on the pure glue part of the brown muck. However, the formalism described above is so general that one could also use it in a LF calculation that includes (dynamical) light quarks.

- 
- [1] P. A. M. Dirac, *Rev. Mod. Phys.* **21**, 392 (1949).  
 [2] X. Ji, *Comments Nucl. Part. Phys.* **21**, 123 (1993).  
 [3] K. G. Wilson *et al.*, *Phys. Rev. D* **49**, 6720 (1994).  
 [4] S. J. Brodsky and D. G. Robertson, in *Proceedings of “ELFE Summer School on Confinement Physics,”* Cambridge, England, 1995, edited by S. D. Bass and P. A. M. Guichon (Editions Frontieres, Gif-sur-Yvette, 1996); Report No. hep-ph/9511374 (unpublished).  
 [5] M. Burkardt, *Adv. Nucl. Phys.* **23**, 1 (1996).  
 [6] W. A. Bardeen and R. B. Pearson, *Phys. Rev. D* **14**, 547 (1976); W. A. Bardeen, R. B. Pearson, and E. Rabinovici, *ibid.* **21**, 1037 (1980).  
 [7] P. A. Griffin, *Mod. Phys. Lett. A* **7**, 601 (1992); P. A. Griffin, *Nucl. Phys.* **B372**, 270 (1992).  
 [8] P. A. Griffin, *Phys. Rev. D* **47**, 1530 (1993).  
 [9] P. A. Griffin, in *Theory of Hadrons and Light Front QCD*, Proceedings of the 4th International Workshop on Light Cone Quantization and Non-Perturbative Dynamics, Polona Zgorzelisko, Poland, 1994, edited by S. Glazek (World Scientific, Singapore, 1994), Report No. hep-ph/9410243 (unpublished).  
 [10] M. Burkardt, in *Proceedings of “ELFE Summer School on Confinement Physics”* [4], Report No. hep-ph/9510264 (unpublished).  
 [11] M. Burdardt and A. Langnau, *Phys. Rev. D* **44**, 3857 (1991).  
 [12] B. Grossmann *et al.*, *Int. J. Mod. Phys. A* **6**, 2649 (1991).  
 [13] M. Burkardt, in *Theory of Hadrons and Light Front QCD* [9], Report No. hep-ph/9410219 (unpublished).  
 [14] H.-C. Pauli and S. J. Brodsky, *Phys. Rev. D* **32**, 1993 (1985); **32**, 2001 (1985).  
 [15] A. C. Kalloniatis, H.-C. Pauli, and S. Pinsky, *Phys. Rev. D* **50**, 6633 (1994); M. Engelhardt and B. Schreiber, *Z. Phys. A* **351**, 71 (1995).  
 [16] K. Hornbostel, *Phys. Rev. D* **45**, 3781 (1992).  
 [17] D. G. Robertson, *Phys. Rev. D* **47**, 2549 (1993).  
 [18] M. Burdardt, *Phys. Rev. D* **47**, 4628 (1993).  
 [19] E. V. Prokhvatilov and V. A. Franke, *Sov. J. Nucl. Phys.* **49**, 688 (1989); E. V. Prokhvatilov, H. W. L. Naus, and H.-J. Pirner, *Phys. Rev. D* **51**, 2933 (1995); J. P. Vary and T. J. Fields, *Theory of Hadrons and Light Front QCD* [9], Report No. hep-ph/9411263 (unpublished).  
 [20] R. J. Perry, in *Hadron Physics 94: Topics on the Structure and Interaction of Hadronic Systems*, Proceedings of the Workshop, Gramado, Brazil, 1994, edited by V. E. Herscovitz *et al.* (World Scientific, Singapore, 1995), Report No. hep-ph/9407056 (unpublished).  
 [21] M. Burkardt, *Phys. Rev. D* **54**, 2913 (1996).  
 [22] F. Lenz, S. Levit, M. Thies, and K. Yazaki, *Ann. Phys. (N.Y.)* **208**, 1 (1991); F. Lenz, in *Proceedings of NATO Advanced Study Institute on Hadrons and Hadronic Matter*, edited by D. Vautherin *et al.* (Plenum, New York, 1990); D. G. Robertson and G. McCartor, *Z. Phys. C* **53**, 661 (1992); A. C. Kalloniatis and H.-C. Pauli, *ibid.* **60**, 255 (1993); **63**, 161 (1994); A. C. Kalloniatis and D. G. Robertson, *Phys. Rev. D* **50**, 5262 (1994); S. S. Pinsky *et al.*, *ibid.* **48**, 816 (1993); **49**, 2001 (1994); **51**, 726 (1995); T. Heinzl *et al.*, *Z. Phys. C* **56**, 415 (1992).  
 [23] B. van de Sande and M. Burkardt, *Phys. Rev. D* **53**, 4628 (1996).  
 [24] B. van de Sande and S. Dalley, Report No. hep-ph/9602291 (unpublished).  
 [25] F. Antonuccio and S. Dalley, *Nucl. Phys.* **B461**, 275 (1996).  
 [26] J. Hiller, *Phys. Rev. D* **43**, 2418 (1991).  
 [27] M. Burkardt, *Phys. Rev. D* **46**, R1924 (1992); **46**, R2751 (1992).  
 [28] M. Burkardt, *Nucl. Phys.* **B373**, 613 (1992).  
 [29] S. D. Glazek and R. J. Perry, *Phys. Rev. D* **45**, 3734 (1992).  
 [30] M. Burkardt, *Phys. Rev. D* **49**, 5446 (1994).  
 [31] M. Burkardt and B. Klindworth (in preparation).